Hindawi
Wireless Communications and Mobile Computing
Volume 2021, Article ID 9892683, 1 page
https://doi.org/10.1155/2021/9892683

Retraction

Retracted: Adaptive Blind Channel Estimation for MIMO-OFDM Systems Based on PARAFAC

Wireless Communications and Mobile Computing

Received 29 April 2021; Accepted 29 April 2021; Published 24 May 2021

Wireless Communications and Mobile Computing has retracted the article titled "Adaptive Blind Channel Estimation for MIMO-OFDM Systems Based on PARAFAC" [1], due to a high level of similarity identified with a previously published article, as confirmed by the editorial board [2]:

Ruo-Nan Yang, Wei-Tao Zhang, Shun-Tian Lou, "Joint Adaptive Blind Channel Estimation and Data Detection for MIMO-OFDM Systems", Wireless Communications and Mobile Computing, vol. 2020, Article ID 2508130, 9 pages, 2020. doi:10.1155/2020/2508130.

The authors do not agree to the retraction.

References

[1] R.-N. Yang, W.-T. Zhang, and S.-T. Lou, "Adaptive Blind Channel Estimation for MIMO-OFDM Systems Based on PARAFAC," *Wireless Communications and Mobile Computing*, vol. 2020, Article ID 8396930, 17 pages, 2020.

[2] R.-N. Yang, W.-T. Zhang, and S.-T. Lou, "Joint Adaptive Blind Channel Estimation and Data Detection for MIMO-OFDM Systems," *Wireless Communications and Mobile Computing*, vol. 2020, Article ID 2508130, 9 pages, 2020.

Hindawi
Wireless Communications and Mobile Computing
Volume 2020, Article ID 8396930, 17 pages
https://doi.org/10.1155/2020/8396930

Research Article

Adaptive Blind Channel Estimation for MIMO-OFDM Systems Based on PARAFAC

Ruo-Nan Yang, Wei-Tao Zhang, and Shun-Tian Lou

School of Electronic Engineering, Xidian University, Xi'an 710071, China

Correspondence should be addressed to Wei-Tao Zhang; zhwt-work@foxmail.com

Received 11 January 2020; Revised 18 August 2020; Accepted 25 September 2020; Published 24 October 2020

Academic Editor: Jun Cai

In order to track the changing channel in multiple-input multiple-output orthogonal frequency division multiplexing (MIMO-OFDM) systems, it is prior to estimate channel impulse response adaptively. In this paper, we proposed an adaptive blind channel estimation method based on parallel factor analysis (PARAFAC). We used an exponential window to weight the past observations; thus, the cost function can be constructed via a weighted least squares criterion. The minimization of the cost function is equivalent to the decomposition of third-order tensor which consists of the weighted OFDM data symbols. To reduce the computational load, we adopt a recursive singular value decomposition method for tensor decomposition; then, the channel parameters can be estimated adaptively. Simulation results validate the effectiveness of the proposed algorithm under diverse signalling conditions.

1. Introduction

The combination of MIMO with OFDM technique has become the most promising broadband wireless access scheme due to large system capacity and high data rates without any extra consumption of bandwidth and power [1]. In a MIMOOFDM system, the channel needs to be estimated accurately, and then, the transmitted signal can be obtained by channel equalization. Thus, an exact estimation of the changing channel impulse response is necessary [2–5].

In the past decades, many methods have been proposed for MIMO-OFDM systems to solve channel estimation problems. They were grouped into two categories. In one of the categories, the channel parameters can be estimated by sending training sequence or inserting pilot structure which is known to the receiver. Especially, one can realize adaptive channel estimation (ACE) by repeating this process periodically [6–13]. Linear channel estimation methods in [14, 15] use an adaptive filter to estimate channel information. Due to less computational complexity, linear channel estimation methods such as least squares (LS) algorithms are relatively easy to implement. The Least Mean Square (LMS) algorithm is one of the ACE methods with relatively low computational complexity, but the mean squared error (MSE) performance is poor [14]. Furthermore, simplified LMS algorithms like the Sign Data NLMS (SDNLMS) algorithm [15] can be used to decrease the complexity of the LMS algorithm. Sparse channel estimation methods [16–20] commonly use the technique of compressive sensing. However, these methods have great dependence on the number of nonzeros taps. The remaining category is semiblind or blind channel estimation [21]. Here, training sequences and knowledge of noise statistics are not necessary; channel impulse response can be estimated only by the received signals. Therefore, blind channel estimation methods have attracted wide attention due to its improved spectral efficiency. Blind channel estimation methods usually use the statistical properties of received signals; channel is considered static during the receiving time. When ACE process is concerned, existing blind OFDM channel estimation methods are not suitable for online applications.

Parallel factor (PARAFAC) analysis has become a useful tool for dealing with linear algebra of multiplexed arrays [22]. In the field of signal processing, PARAFAC has been widely used for blind signal detection and parameter estimation. In

many recent works, tensor decompositions are used for blind channel estimation in OFDM systems [23–27]. [24] proposed a trilinear alternating least squares (TALS) algorithm to estimate channel parameters for SIMO-OFDM systems with Carrier Frequency Offset (CFO). However, the extension on MIMO-OFDM systems is missed. The TALS method can obtain good MSE, but it has high computational complexity and poor convergence rate. The DEterministic Blind REceiver (DEBRE) algorithm uses the received signal to form a 4-way tensor for MIMO-OFDM system in frequency domain; then, the parameters of the model are identified via an ALS algorithm [25]. Similar with the TALS algorithm, the computational complexity of the DEBRE method is very high. The least squares Khatri-Rao factorization (LS-KRF) algorithm and simplified closed-form PARAFAC (S-CFP) algorithm are established based on the tensor model for Tucker decomposition [26], and they achieve very similar performance with extra pilot overhead at high signal-to-noise ratio (SNR) conditions. The mentioned algorithms on PARAFAC are suitable for stationary channel environment; when the tensor model needed to be decomposed at each sampling instant, the computation complexity is too high.

There are some existing fast adaptive PARAFAC decomposition algorithms in mathematics [28, 29]. The two recursive update algorithms in [28] use a sliding or an exponential window to weight the observations, the computation complexities are very low. The 3DOPAST algorithm generalizes the orthonormal projection approximation subspace tracking (OPAST) method to track the loading matrix of third-order tensor [29]. However, none of them are used for adaptive channel estimation of MIMO-OFDM systems. In this paper, we proposed an online adaptive blind channel estimation method using simultaneous diagonalization tracking. We use an exponential window to weight past observations; thus, the cost function can be constructed via a least squares criterion. We construct a third-order tensor which is composed by all the observations; the third loading matrix of the tensor can span the same column space with the right singular matrix of the weighted matrix. Therefore, we can obtain a nonsingular matrix to link them. By updating the nonsingular matrix, the channel parameters can be estimated adaptively. Different from many existing methods that only use the last receiving symbols to estimate current channel, the proposed cost function involves the past information of the exponential windowed receiving signals; thus, we can obtain better performance than the existing methods.

The remainder of this paper is organized as follows. In Section 2, we introduced the PARAFAC-based MIMO-OFDM system model. In Section 3, an adaptive channel estimation algorithm is developed for tracking changing channels in MIMO-OFDM systems. Simulation results are presented in Section 4. Finally, our conclusions are given in Section 5. The main contribution of this paper is briefly summarized as follows: (1) we propose a PARAFAC model for time-varying MIMO-OFDM systems in time domain, where time is measured in OFDM symbols. For one OFDM symbol, by reshaping the received signal vector of all antennas, and letting the reshaped matrix be the lateral slice matrix one by one, we establish a third-order tensor model for time-varying MIMO-OFDM systems. (2) We develop an adaptive channel estimation algorithm using simultaneous diagonalization tracking (ABCE-SDT). Here, training sequences and knowledge of noise statistics are not necessary; channel impulse response can be estimated adaptively only by the received signals. In addition, our algorithm is a recursive update solution; the computation complexity is very low compared to other PARAFAC decomposition counterpart. (3) We compare the performance of the proposed algorithm with other existing channel estimation methods. Simulation results show that compared with the SDNLMS algorithm and adaptive sparse channel estimation (ASCE-NLMS) algorithm, the proposed algorithms can significantly improve the channel estimation performance of time-varying systems under different conditions.

Notation: scalars are denoted by lower case italic letters $(a, b, \cdots)$, vectors by lower case boldface letters $(\mathbf{a}, \mathbf{b}, \cdots)$, and matrices by boldface capitals $(\mathbf{A}, \mathbf{B}, \cdots)$. Italic capitals are used to denote index upper bound $(k = 1, \cdots, K)$. The entry with row index i and column index j in a matrix $\mathbf{A}$, i.e., $[\mathbf{A}]_{ij}$, is symbolized by a_{ij}. The columns of a matrix, say $\mathbf{A}$, are denoted by $\mathbf{a}_1, \mathbf{a}_2, \cdots$ generically. The superscripts $\cdot^T$, $\cdot^H$, $\cdot^{-1}$, and $\cdot^\dagger$ denote the transpose, conjugate transpose, inverse operators, and pseudo inverse, respectively. $\mathbf{I}_N$ denotes the $N \times N$ identity matrix; $\|\cdot\|_2$ denotes the Euclid norm. $\odot$ denotes the Khatri-Rao product. $E[\cdot]$ denotes the expectation operator. The operator diag $(\cdot)$ may either forms a diagonal matrix by a vector or forms a vector by collecting the diagonal entries of a matrix.

2. System Model

In this section, we describe the MIMO-OFDM system model with M_t transmit antennas and M_r receive antennas. N symbols are transmitted in each OFDM block, so the kth modulated information of ith transmitter is $\mathbf{s}_i(k) = [s_i(k, 0), \cdots, s_i(k, N-1)]^T$. Suppose all the $M_t \times M_r$ channel paths have the memory upper bounded by L, and let $\tilde{\mathbf{h}}_{ij}^T = [\tilde{h}_{ij}(1), \tilde{h}_{ij}(2), \cdots, \tilde{h}_{ij}(L-1)]$ denote the equivalent discrete channel response from the ith transmit antenna to the jth receive antenna. So the N points DFT of the channel vector is $\mathbf{h}_{ij}^T = [h_{ij}(1), h_{ij}(2), \cdots, h_{ij}(N)]$. The received signal vector from the jth receive antenna by the ith transmit antenna is then represented as

$$\mathbf{x}_{ij}(k) = \mathbf{F}^H \text{ diag } (\mathbf{h}_{ij}) \mathbf{s}_i(k), \tag{1}$$

where $\mathbf{F}$ denotes the $N \times N$ normalized discrete Fourier transform matrix with its (m, q)-th entry given by $(1/\sqrt{N})$ $e^{-j2\pi(m-1)(q-1)}$.

Let

$$\mathbf{H} = \begin{bmatrix} \mathbf{h}_{11}^T & \mathbf{h}_{21}^T & \cdots & \mathbf{h}_{M_t 1}^T \\ \mathbf{h}_{12}^T & \mathbf{h}_{22}^T & \cdots & \mathbf{h}_{M_t 2}^T \\ \vdots & \vdots & \ddots & \vdots \\ \mathbf{h}_{1M_r}^T & \mathbf{h}_{2M_r}^T & \cdots & \mathbf{h}_{M_t M_r}^T \end{bmatrix} \in \mathbb{C}^{M_r \times M_t N} \tag{2}$$

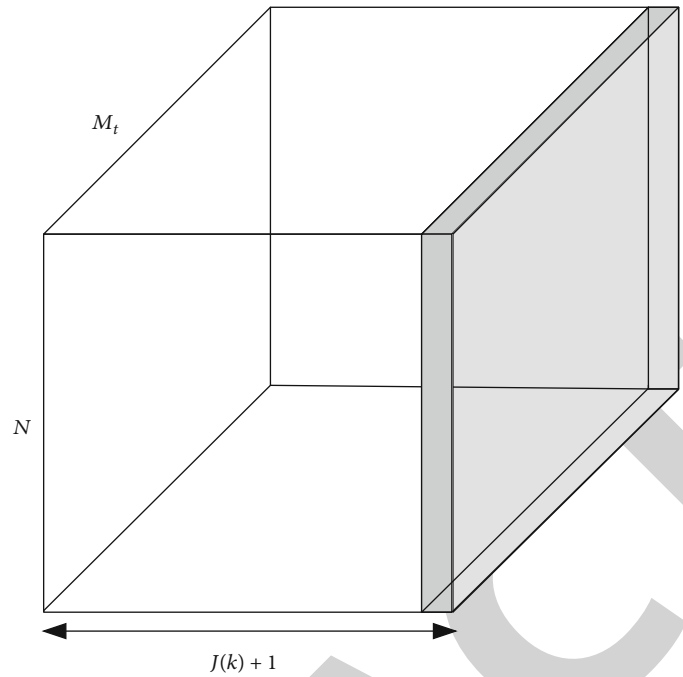

Figure 1: Appending a new slice in the tensor of observation.

denote the overall frequency-domain channel matrix. Therefore, the received symbol vector $\mathbf{x}_j(k) = \sum_{i=1}^{M_t} \mathbf{x}_{ij}(k)$ from the j th receive antenna is

$$\mathbf{x}_j(k) = \sum_{i=1}^{M_t} \mathbf{F}^H \operatorname{diag}\left(\mathbf{h}_{ij}\right)\mathbf{s}_i(k). \tag{3}$$

Constructing the matrix $\boldsymbol{\Gamma} = [\mathbf{I}_N \ \mathbf{I}_N \ \cdots \ \mathbf{I}_N] \in \mathbb{C}^{N\times NM_t}$, $\mathbf{x}_j(k)$ can be represented as

$$\mathbf{x}_j(k) = \mathbf{F}^H \boldsymbol{\Gamma} \boldsymbol{D}_j(\mathbf{H})\mathbf{s}(k), \tag{4}$$

where $\mathbf{s}(k) = [\mathbf{s}_1(k)^T, \mathbf{s}_2(k)^T, \cdots, \mathbf{s}_{M_t}(k)^T]^T \in \mathbb{C}^{NM_t\times 1}$, $\boldsymbol{D}_j(\mathbf{H})$ denote the diagonal matrix with its entries from the jth row of the frequency-domain channel matrix $\mathbf{H}$. Now, we consider a time-varying MIMO-OFDM system. Suppose that the channel parameters stay unchanged during one OFDM symbol and vary for different OFDM symbols. Therefore, we define the channel matrix at the kth symbols as $\mathbf{H}(k)$. Considering all the M_r receive antennas, the received signal vector of all antennas $\mathbf{x}(k) = [\mathbf{x}_1(k)^T, \mathbf{x}_2(k)^T, \cdots, \mathbf{x}_{M_r}(k)^T]^T \in \mathbb{C}^{NM_r\times 1}$ is then represented as

$$\mathbf{x}(k) = \left[\mathbf{H}(k) \odot \left(\mathbf{F}^H \boldsymbol{\Gamma}\right)\right]\mathbf{s}(k). \tag{5}$$

If we reshape $\mathbf{x}(k)$ to be a $N \times M_r$ matrix, then we stack up corresponding matrices of $J(k)$ OFDM symbols, a third-order tensor $\mathcal{X}(k) \in \mathbb{C}^{N\times J(k)\times M_r}$ can be obtained, which is composed by all the receive symbols.

As we know, the PARAFAC decomposition of a third-order tensor $\mathcal{Y} \in \mathbb{C}^{I\times J\times K}$ is a decomposition of $\mathcal{Y}$ as a sum of minimal number of rank-1 tensors

$$\mathcal{Y} = \sum_{r=1}^{R} \mathbf{a}_r \circ \mathbf{b}_r \circ \mathbf{c}_r, \tag{6}$$

where $\mathbf{a}_r$, $\mathbf{b}_r$, and $\mathbf{c}_r$ are the rth columns of $\mathbf{A} \in \mathbb{C}^{I\times R}$, $\mathbf{B} \in \mathbb{C}^{J\times R}$, and $\mathbf{C} \in \mathbb{C}^{K\times R}$, respectively [28]. **A**, **B**, and **C** are named "loading matrices." The matrix representations of the tensor decomposition are as follows:

$$\begin{cases} \mathbf{Y}^{(JK\times I)} = (\mathbf{C} \odot \mathbf{B})\mathbf{A}^T \\ \mathbf{Y}^{(KI\times J)} = (\mathbf{A} \odot \mathbf{C})\mathbf{B}^T \\ \mathbf{Y}^{(IJ\times K)} = (\mathbf{B} \odot \mathbf{A})\mathbf{C}^T \end{cases}. \tag{7}$$

Therefore, matrix representation of tensor decomposition of $\mathcal{X}(k)$ can be written as

$$\mathbf{X}(k) = \left[\mathbf{H}(k) \odot \left(\mathbf{F}^H \boldsymbol{\Gamma}\right)\right]\mathbf{S}(k), \tag{8}$$

where $\mathbf{X}(k) = [\mathbf{x}(1), \cdots, \mathbf{x}(J(k))] \in \mathbb{C}^{NM_r\times J(k)}$, $\mathbf{S}(k) = [\mathbf{s}(1), \cdots, \mathbf{s}(J(k))]$ denote the continuous $J(k)$ transmit symbols. Since the matrix $\mathbf{F}$ and $\boldsymbol{\Gamma}$ are both constant, we define $\mathbf{A} = \mathbf{F}^H\boldsymbol{\Gamma}$ for derivation clarity, then (8) can be rewritten as $\mathbf{X}(k) = [\mathbf{H}(k) \odot \mathbf{A}]\mathbf{S}(k)$. Thus, the loading matrices are $\mathbf{H}(k) \in \mathbb{C}^{M_r\times NM_t}$, $\mathbf{S}(k) \in \mathbb{C}^{NM_t\times J(k)}$, and $\mathbf{A} \in \mathbb{C}^{N\times NM_t}$, respectively. Therefore, we can obtain the channel information by solving the loading matrices of the tensor.

Input: Old estimations: $\mathbf{S}(k)$, $\mathbf{W}_w(k)$, $\mathbf{Q}_w(k)$ and $\mathbf{V}(k)$
Observations: $\mathbf{X}(k)$ and $\mathbf{X}(k+1) = [\mathbf{X}(k), \mathbf{x}(k+1)]$
1: SVD
First option: Do SVD of $\mathbf{X}(k+1)$
Outputs: $\mathbf{U}_w(k+1)$, $\sum_w(k+1)$ and $\mathbf{V}_w(k+1)$
2: Updates $\mathbf{W}_w$ and $\mathbf{P}_w$
Build matrices:
$\tilde{\mathbf{V}}(k) = \mathbf{V}_w(k)$, $\bar{\mathbf{V}}(k) = [\mathbf{V}_w(k+1)]_{1:J(k)}$,:
$\tilde{\mathbf{v}}(k+1) = [\mathbf{V}_w(k+1)]_{J(k+1)}$,:
$\mathbf{z} = \lambda^{-1/2}\bar{\mathbf{V}}^H(k+1)\tilde{\mathbf{V}}(k)$
Update $\mathbf{W}_w$:
$\mathbf{W}_w(k+1) = \mathbf{Z}\mathbf{W}_w(k)$
Update $\mathbf{P}_w$:
$\mathbf{P}_w(k+1) = \mathbf{P}_w(k)\mathbf{Z}^H(\mathbf{I}_{NM_t}(\tilde{\mathbf{v}}^H(k+1)\tilde{\mathbf{v}}(k+1)/1 - \|\tilde{\mathbf{v}}(k+1)\|^2))$
3: Update H
$\mathbf{G}(k+1) = \mathbf{Q}_w(k+1)\mathbf{W}_w(k+1)$
$\mathbf{A} = \mathbf{F}^H\boldsymbol{\Gamma}$, $R = NM_t$
For $r = 1 \cdots R$ Do
$\mathbf{G}_r(k+1) = \text{Unvec}_{N\times M_r}([\mathbf{G}(k+1)]_{:,r})$
$\hat{\mathbf{h}}_r(k+1) = \mathbf{G}_r^T(k+1)\mathrm{a}_r^*$
End
$\hat{\mathbf{H}}(k+1) = [\hat{\mathbf{h}}_1(k+1), \hat{\mathbf{h}}_2(k+1), \cdots, \hat{\mathbf{h}}_R(k+1)]$
4: Update S$(k+1)$
$\hat{\mathbf{s}}(k+1) = \mathbf{P}_w(k+1)\tilde{\mathbf{v}}^H(k+1)$
$\hat{\mathbf{S}}(k+1) = [\mathbf{S}(k)\hat{\mathbf{s}}(k+1)]$
Output: Matrices $\hat{\mathbf{H}}(k+1)$ and $\hat{\mathbf{S}}(k+1)$ now stand for estimations of the channel and signals respectively.

Algorithm 1:Proposed ABCE-SDT Algorithm.

3. Blind Adaptive Channel Estimation Algorithm

3.1. Uniqueness Analysis. The CP decomposition of a tensor is unique up to scaling and permutation ambiguities under a mild condition [28, 30]. The PARAFAC decomposition of $\mathcal{X} \in \mathbb{C}^{I\times J\times K}$ is said to be essentially unique if any other matrix triplet $(\tilde{\mathbf{A}}, \tilde{\mathbf{B}}, \tilde{\mathbf{C}})$ that also satisfy the model is related to $(\mathbf{A}, \mathbf{B}, \mathbf{C})$ via

$$\mathbf{A} = \tilde{\mathbf{A}}\boldsymbol{\Pi}\boldsymbol{\Lambda}_1, \mathbf{B} = \tilde{\mathbf{B}}\boldsymbol{\Pi}\boldsymbol{\Lambda}_2, \mathbf{C} = \tilde{\mathbf{C}}\boldsymbol{\Pi}\boldsymbol{\Lambda}_3, \tag{9}$$

with $\boldsymbol{\Lambda}_1$, $\boldsymbol{\Lambda}_2$, and $\boldsymbol{\Lambda}_3$ arbitrary diagonal matrices satisfying $\boldsymbol{\Lambda}_1\boldsymbol{\Lambda}_2\boldsymbol{\Lambda}_3 = \mathbf{I}_R$, and $\boldsymbol{\Pi}$ is an arbitrary permutation matrix. A specific case is where two loading matrices are full column rank, and the third one does not contain collinear columns. In this case, PARAFAC is unique up to its trivial indeterminacies. This result is summarized in the following Theorem [28].

Theorem 1. *Assume $\mathbf{A} \in \mathbb{C}^{I\times R}$ and $\mathbf{C} \in \mathbb{C}^{I\times R}$ are drawn from a jointly continuous distribution with respect to the Lebesgue measure in $\mathbb{C}^{I\times R+K\times R}$, and $\mathbf{B} \in \mathbb{C}^{J\times R}$ is full column rank. The PARAFAC decomposition of $\mathcal{X}$ is essentially unique if*

$$R \le K \text{ and } R(R-1) \le I(I-1)J(J-1)/2. \tag{10}$$

According to the Theorem 1, we can obtain a similar Lemma 2 about the CP decomposition of the tensor for MIMO-OFDM systems.

Lemma 2. *Assume that $\mathbf{A}$ and $\mathbf{H}(k)$ are full rank, and $\mathbf{S}(k)$ is full column rank. The CP decomposition in (8) is essentially unique if*

$$NM_t(NM_t - 1) \le N(N-1)J(k)(J(k)-1)/2. \tag{11}$$

The above assumptions are generically satisfied in our signal model. On one hand, the normalized discrete Fourier transform matrix is full rank, and then, the channel matrix is completely full rank surely. On the other hand, all the transmit signals are assumed to have independent continuous distribution; thus, the symbols matrix $\mathbf{S}(k)$ is full column rank, which practically satisfies Lemma 2.

3.2. The Algorithm Derivation. We use the first $J(k)$ receiving symbols to build the initial observed tensor $\mathcal{X}(k)$. As illustrated in Figure 1, let $\mathcal{X}(k+1) \in \mathbb{C}^{N\times J(k+1)\times M_r}$ be the new observation after attaching a new received signal tensor as the side slice of $\mathcal{X}(k)$, which means that $J(k+1) = J(k) + 1$. Similar to (8), the PARAFAC decomposition of $\mathcal{X}(k+1)$ is

$$\mathbf{X}(k+1) = \mathbf{G}(k+1)\mathbf{S}(k+1), \tag{12}$$

where $\mathbf{G}(k+1) = \mathbf{H}(k+1) \odot \mathbf{A}$.

In fact, the alternating least squares (ALS) algorithm can be used to do PARAFAC decomposition of $\mathcal{X}(k+1)$ [24].

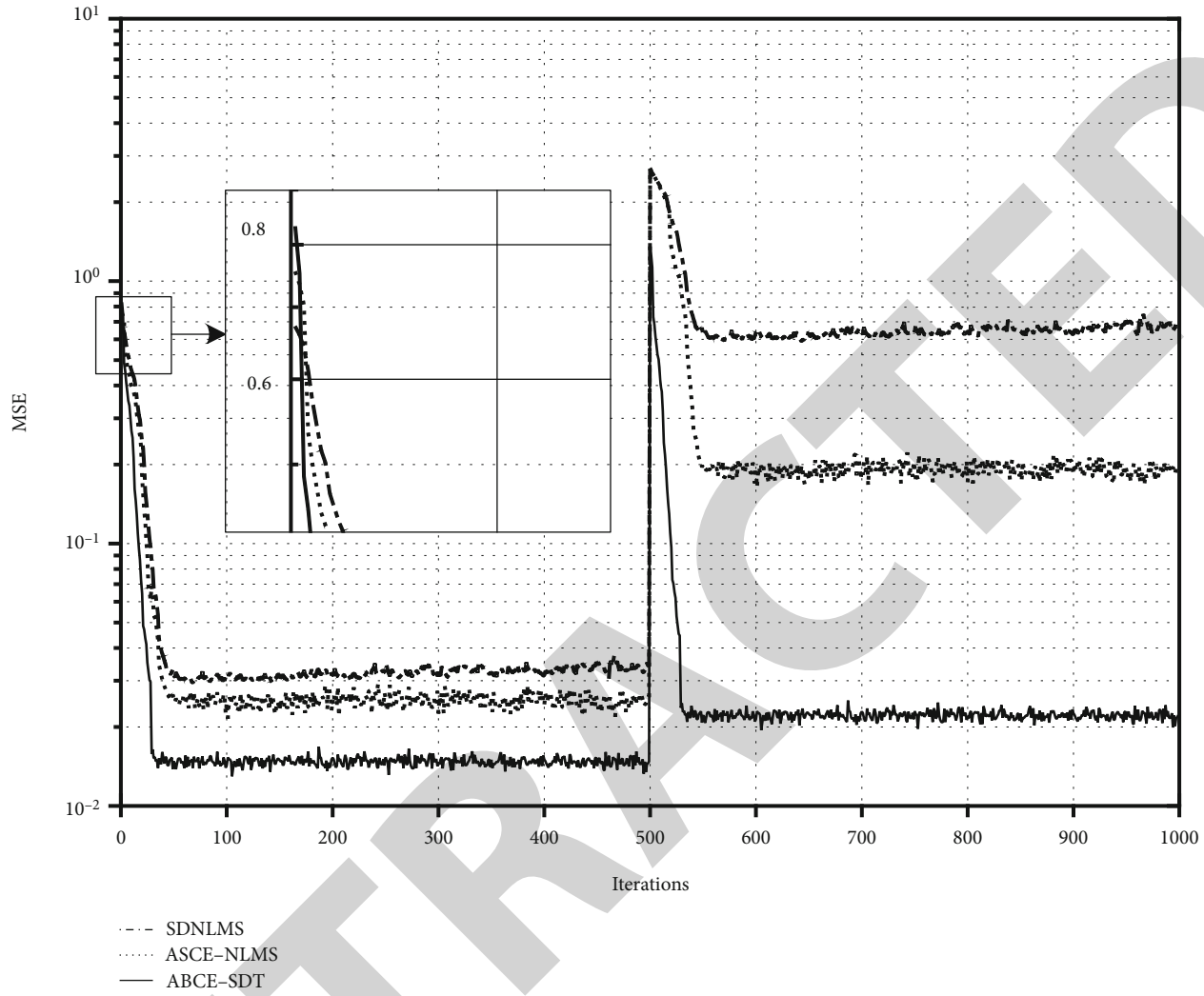

Figure 2: Channel estimation performances of three algorithms.

However, the ALS algorithm needs to do pseudoinverse operation three times in each iteration, and the convergence speed is very slow even with a proper initialization. When it is necessary to decompose the tensor model at each sampling time, the computation complexity is too high. Here, we proposed a closed form solution to avoid the drawbacks of the iterative ALS algorithm. An exponential window least squares criterion is adopted, and the resulting algorithm does not require iterations for channel estimation in one OFDM symbol period. In addition, we avoid directly performing the optimization of the cost function; the minimization of the cost function is transformed to the decomposition of third-order tensor which consists of the weighted OFDM data symbols; thus, the computational complexity can be reduced.

Let $\mathbf{x}(k+1) \in \mathbb{C}^{NM_r \times 1}$ be the new lateral slice appended to $\mathcal{X}(k)$, such that $\mathbf{X}(k+1) = [\mathbf{X}(k) \quad \mathbf{x}(k+1)]$. Suppose that there is a mild variation of channel parameters between k to $k+1$, which means $\mathbf{H}(k) \simeq \mathbf{H}(k+1)$. So the initial estimate of $\mathbf{s}(k+1)$ can be given in the least squares sense by $\mathbf{s}(k+1) = \mathbf{G}^{\dagger}(k)\mathbf{x}(k+1)$; then, the estimation of symbols $\mathbf{S}(k+1)$ can be built as the structure $\mathbf{S}(k+1) = [\mathbf{S}(k) \quad \mathbf{s}(k+1)]$. So that the least squares update of $\mathbf{G}(k+1)$ is then given by

$$\mathbf{G}(k+1) = \mathbf{X}(k+1)(\mathbf{S}(k+1))^{\dagger}. \tag{13}$$

Given $\mathbf{G}(k+1)$, then we can reupdate $\mathbf{s}(k+1)$ by substituting $\mathbf{G}(k)$ by $\mathbf{G}(k+1)$. Finally, since $\mathbf{G}(k+1)$ is an estimate for $\mathbf{H}(k+1) \odot \mathbf{A}$, the estimation of $\mathbf{H}(k+1)$ can be obtained. To track the channel in a time-varying MIMO-OFDM system, the sufficient statistic data in (5) should be gradually forgotten. To this end, we use the following exponential window least squares criterion to equal the decomposition of third-order tensor $\mathcal{X}(k+1)$.

$$\min_{\{\mathbf{G}(k+1),\mathbf{S}(k+1)\}} \left(\sum_{\tau=1}^{k+1} \lambda^{k+1-\tau} \|\mathbf{x}(\tau) - \mathbf{G}(k+1)\mathbf{s}(\tau)\|^2 \right), \tag{14}$$

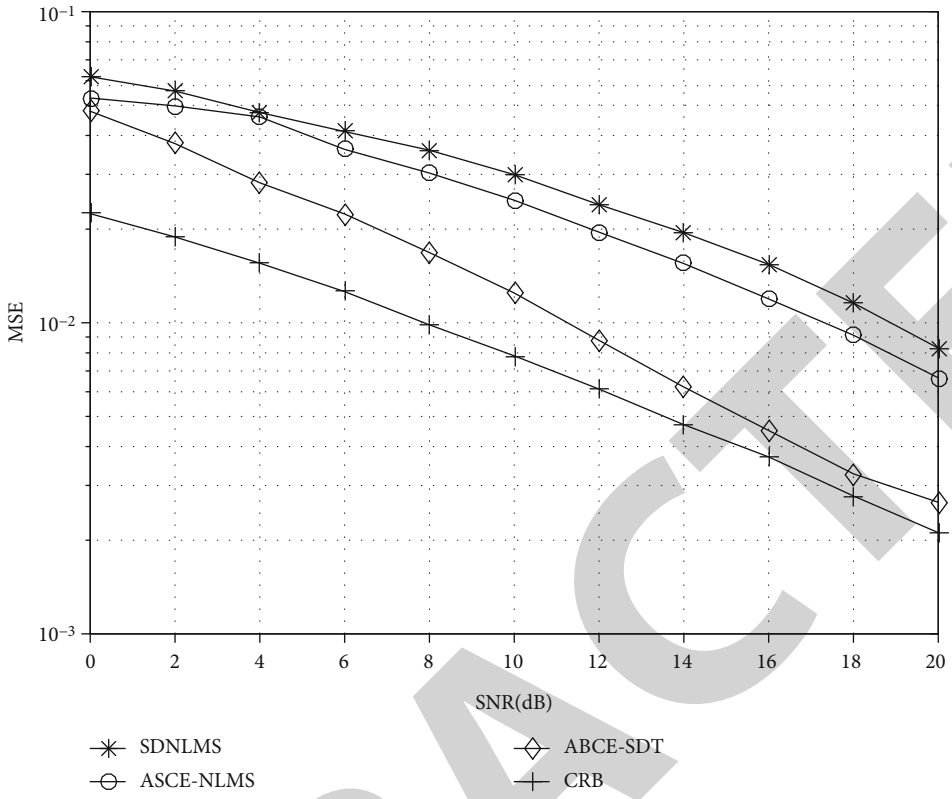

Figure 3: Channel estimation performances with abruptly changing environment.

where $0 < \lambda < 1$ is the forgetting factor. Thus, we define the windowed observed matrix as

$$\mathbf{X}_w(k+1) = \mathbf{X}(k+1)\boldsymbol{\Lambda}(k+1), \tag{15}$$

where $\boldsymbol{\Lambda}(k+1) = \text{diag}([\lambda^{k/2}, \lambda^{k-1/2}, \cdots, \lambda^{1/2}, 1])$ is the weighting matrix. Thus, we can obtain $\mathbf{X}_w(k) = (\mathbf{H}(k) \odot \mathbf{A})\mathbf{S}(k)\boldsymbol{\Lambda}(k)$ based on the PARAFAC decomposition. The exponential window implies the following update rule

$$\mathbf{X}_w(k+1) = \left[\lambda^{1/2}\mathbf{X}_w(k), \mathbf{x}(k+1)\right], \tag{16}$$

then we consider the SVD of the weighted matrix $\mathbf{X}_w(k) = \mathbf{U}_w(k)\boldsymbol{\Sigma}_w(k)\mathbf{V}_w^{\mathrm{H}}(k)$, where $\mathbf{U}_w(k) \in \mathbb{C}^{NM_r \times NM_t}$, $\boldsymbol{\Sigma}_w(k) \in \mathbb{C}^{NM_t \times NM_t}$, and $\mathbf{V}_w(k) \in \mathbb{C}^{J(k) \times NM_t}$. Since the PARAFAC decomposition of $\mathcal{X}(k)$ satisfies the Lemma 2, the weighted matrix $\mathbf{X}_w(k)$ has the same rank with $\mathbf{X}(k)$, which means rank $(\mathbf{X}_w(k)) = NM_t$. To satisfy the condition, we restrict to $J(k) \geq NM_t$ and $M_r \geq M_t$. Therefore, there exists a nonsingular matrix $\mathbf{W}_w(k) \in \mathbb{C}^{NM_t \times NM_t}$ such that

$$\mathbf{H}(k) \odot \mathbf{A} = \mathbf{Q}_w(k)\mathbf{W}_w(k), \tag{17}$$

$$\mathbf{S}(k)\boldsymbol{\Lambda}(k) = \mathbf{W}_w^{-1}(k)\mathbf{V}_w^H(k), \tag{18}$$

where $\mathbf{Q}_w(k) = \mathbf{U}_w(k)\boldsymbol{\Sigma}_w(k)$. It is easy to see that the matrix $\mathbf{W}_w(k)$ links equations (17) and (18). When the $(k+1)$th symbols transmit to the receiver, the equations become

$$\mathbf{H}(k+1) \odot \mathbf{A} = \mathbf{Q}_w(k+1)\mathbf{W}_w(k+1), \tag{19}$$

$$\mathbf{S}(k+1)\boldsymbol{\Lambda}(k+1) = \mathbf{W}_w^{-1}(k+1)\mathbf{V}_w^H(k+1). \tag{20}$$

Hence, we can use the common block between $\mathbf{S}(k)$ and $\mathbf{S}(k+1)$ to update the matrix $\mathbf{W}_w$. To avoid SVD at every k th time, we can perform the classical Bi-Iteration technique to do adaptive SVD of $\mathbf{X}_w(k)$ [31]. By this means, the computational complexity can be decreased. In addition, to avoid explicit computation of the pseudoinverse of $\mathbf{W}_w$, derivation of recursive updates of $\mathbf{W}_w^{-1}$ should be taken into consideration; thus, we define $\mathbf{P}_w = \mathbf{W}_w^{-1}$.

For derivation clarity, we define $\tilde{\mathbf{V}}(k) = \mathbf{V}_w(k)$ and rewrite $\mathbf{V}_w(k+1)$ as

$$\mathbf{V}_w(k+1) = \begin{bmatrix} \bar{\mathbf{V}}(k+1) \\ \tilde{\mathbf{v}}(k+1) \end{bmatrix}, \tag{21}$$

where $\tilde{\mathbf{v}}(k+1)$ is the last row of $\mathbf{V}_w(k+1)$. Based on the structure of $\mathbf{S}(k+1) = [\mathbf{S}(k) \quad \mathbf{s}(k+1)]$, we can obtain the following equation from equations (17) and (19)

$$\lambda^{1/2}\mathbf{P}_w(k)\tilde{\mathbf{V}}^H(k) = \mathbf{P}_w(k+1)\bar{\mathbf{V}}^H(k+1), \tag{22}$$

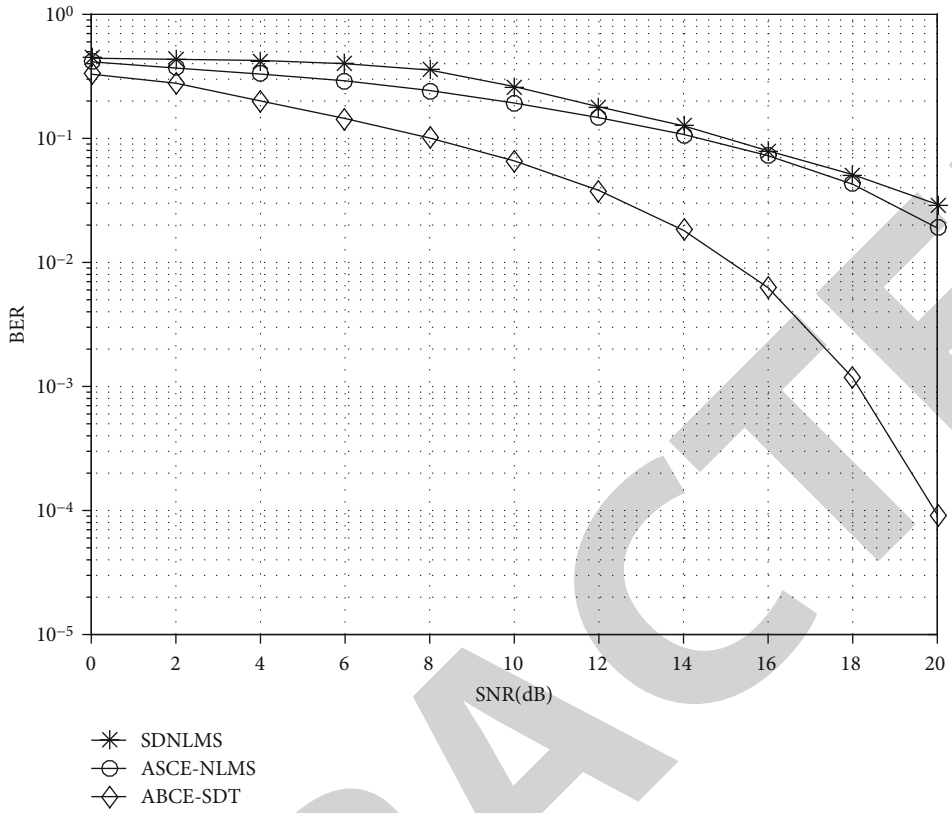

Figure 4: BER performances with abruptly changing environment.

it follows that

$$\mathbf{P}_w(k+1) = \lambda^{1/2}\mathbf{P}_w(k)\tilde{\mathbf{V}}^H(k)\left(\bar{\mathbf{V}}^H(k+1)\right)^{\dagger}, \quad (23)$$

thus, the computation of $\mathbf{W}_w(k+1)$ is

$$\mathbf{W}_w(k+1) = \lambda^{-1/2}\bar{\mathbf{V}}^H(k+1)\left(\tilde{\mathbf{V}}^H(k)\right)^{\dagger}\mathbf{W}_w(k). \quad (24)$$

Obviously, computation of the pseudoinverse of $\tilde{\mathbf{V}}^H(k)$ and $\bar{\mathbf{V}}^H(k+1)$ is not expected in our algorithm. Since $\tilde{\mathbf{V}}(k) = \mathbf{V}_w(k)$ is a unitary matrix, we have $(\tilde{\mathbf{V}}^H(k))^{\dagger} = \mathbf{V}_w(k)$; thus, the computation of $\mathbf{W}_w(k+1)$ can be rewritten as

$$\mathbf{W}_w(k+1) = \lambda^{-1/2}\bar{\mathbf{V}}^H(k+1)\mathbf{V}_w(k)\mathbf{W}_w(k). \quad (25)$$

To avoid explicit computation of the pseudoinverse of $\bar{\mathbf{V}}(k+1)$, derivation of recursive updates of $\bar{\mathbf{V}}(k+1)^{\dagger}$ should be taken into consideration. As the definition of $\bar{\mathbf{V}}(k+1)$ before, we can obtain the following equation from the matrix inversion Lemma for rank-1 updates [28],

$$\left(\bar{\mathbf{V}}^H(k+1)\right)^{\dagger} = \bar{\mathbf{V}}(k+1)\left(\mathbf{I}_{NM_t} + \frac{\tilde{\mathbf{v}}^H(k+1)\tilde{\mathbf{v}}(k+1)}{1-\|\tilde{\mathbf{v}}(k+1)\|^2}\right). \quad (26)$$

Substitute (26) into (23), the computation of $\mathbf{P}_w(k+1)$ is

$$\mathbf{P}_w(k+1) = \lambda^{1/2}\mathbf{P}_w(k)\tilde{\mathbf{V}}^H(k)\bar{\mathbf{V}}(k+1)\left(\mathbf{I}_{NM_t} + \frac{\tilde{\mathbf{v}}^H(k+1)\tilde{\mathbf{v}}(k+1)}{1-\|\tilde{\mathbf{v}}(k+1)\|^2}\right). \quad (27)$$

Therefore, the matrix $\mathbf{G}(k+1) = \mathbf{Q}_w(k+1)\mathbf{W}_w(k+1)$ can be obtained. Let $\hat{\mathbf{H}}(k+1) = [\mathbf{h}_1(k+1), \mathbf{h}_2(k+1), \cdots, \mathbf{h}_R(k+1)]$ as the estimation matrix of the channel, where $R = NM_t$. Due to the Khatri-Rao product $\mathbf{G}(k+1) = \mathbf{H}(k+1) \odot \mathbf{A}$, we can obtain the following equation:

$$\mathbf{g}_r(k+1) = \mathbf{h}_r(k+1) \otimes \mathbf{a}_r, r = 1, 2, \cdots R, \quad (28)$$

where $\mathbf{g}_r(k+1)$ denotes the rth column of $\mathbf{G}(k+1)$, and $\mathbf{a}_r$ denotes the rth column of $\mathbf{A}$. We define the rank-one matrices $\mathbf{G}_r(k+1) = unvec_{M_r \times N}(\mathbf{g}_r(k+1))$, $r = 1, 2, \cdots R$, as

$$\mathbf{G}_r(k+1) = \mathbf{a}_r\mathbf{h}_r^T(k+1). \quad (29)$$

Since the normalized discrete Fourier transform matrix $\mathbf{F}$ and the correlation coefficient matrix $\boldsymbol{\Gamma}$ are constant, we can obtain the equation of rth column of $\mathbf{H}(k+1)$

$$\mathbf{h}_r(k+1) = \mathbf{G}_r^T(k+1)\mathbf{a}_r^*. \quad (30)$$

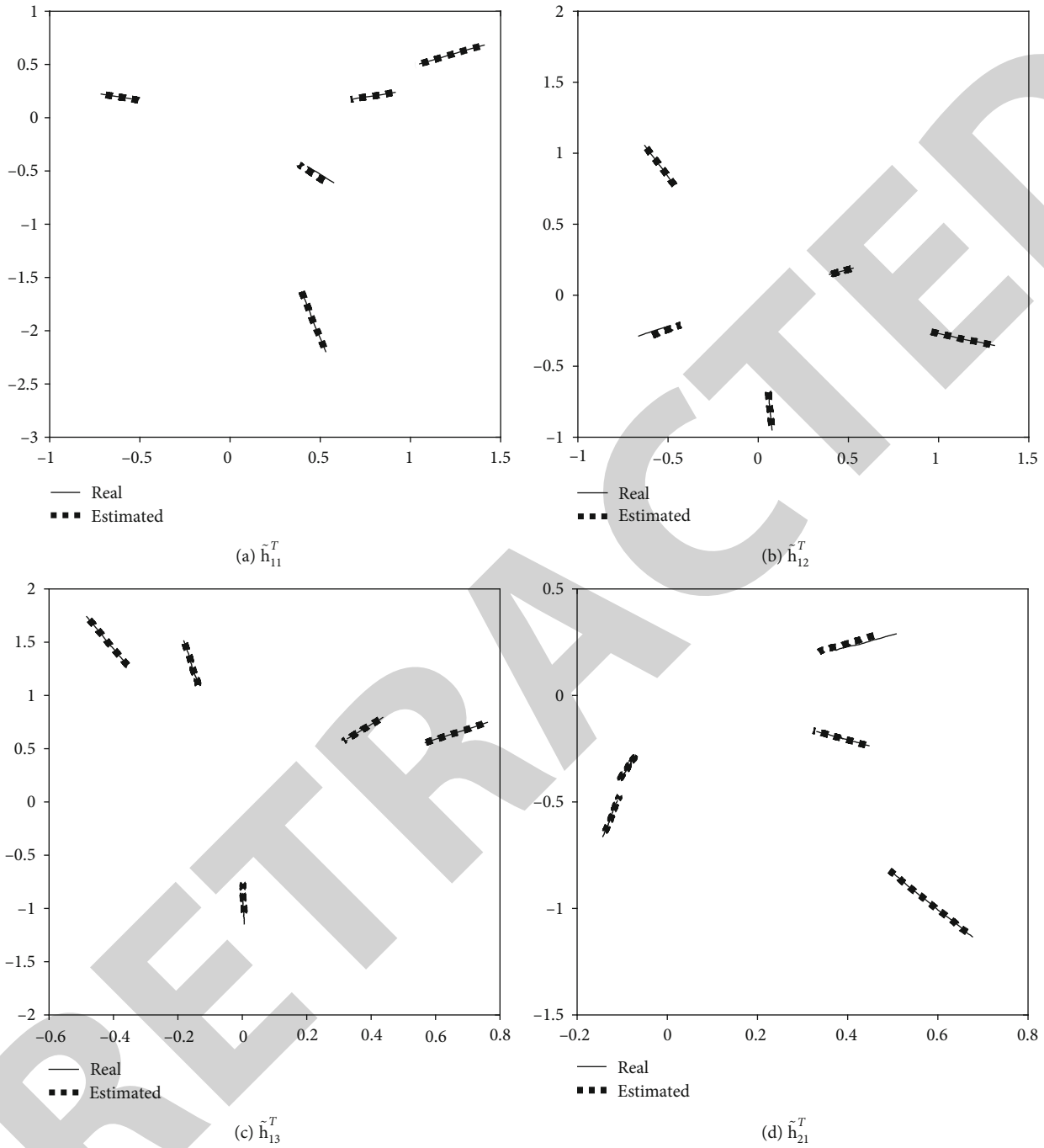

Figure 5: Continued.

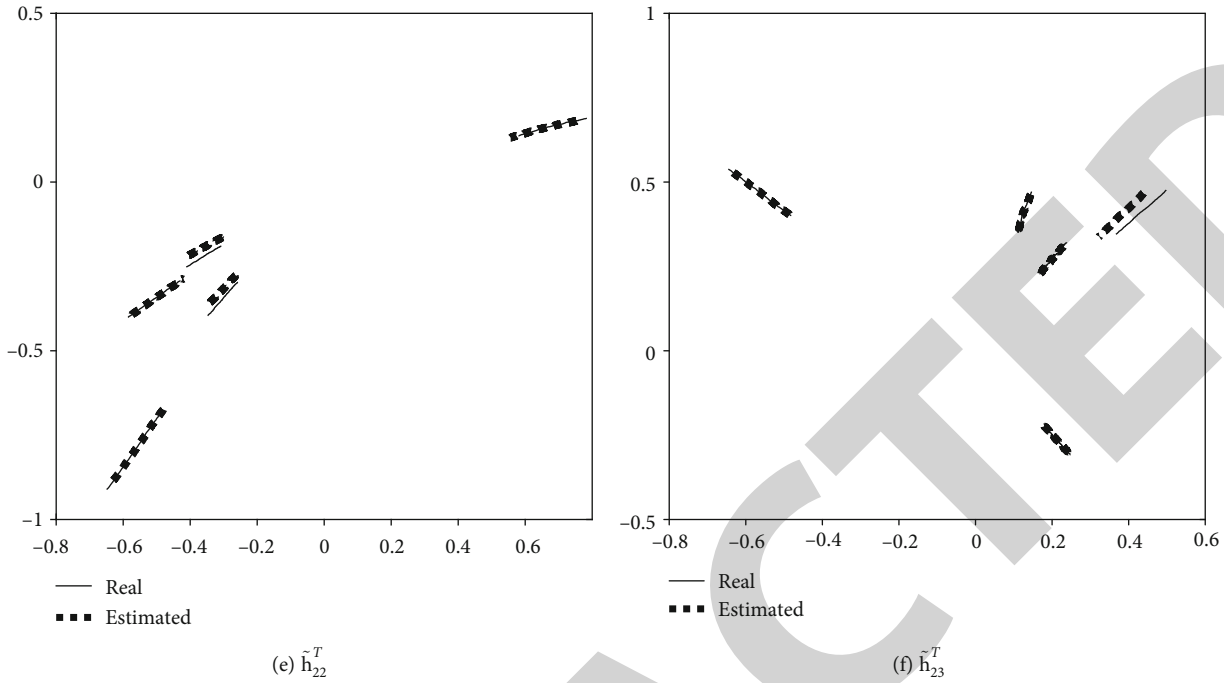

(e) $\tilde{h}_{22}^{T}$ (f) $\tilde{h}_{23}^{T}$

Figure 5: Estimated channel and real linearly changing channel ($M_t = 2$, $M_r = 3$, $L = 5$).

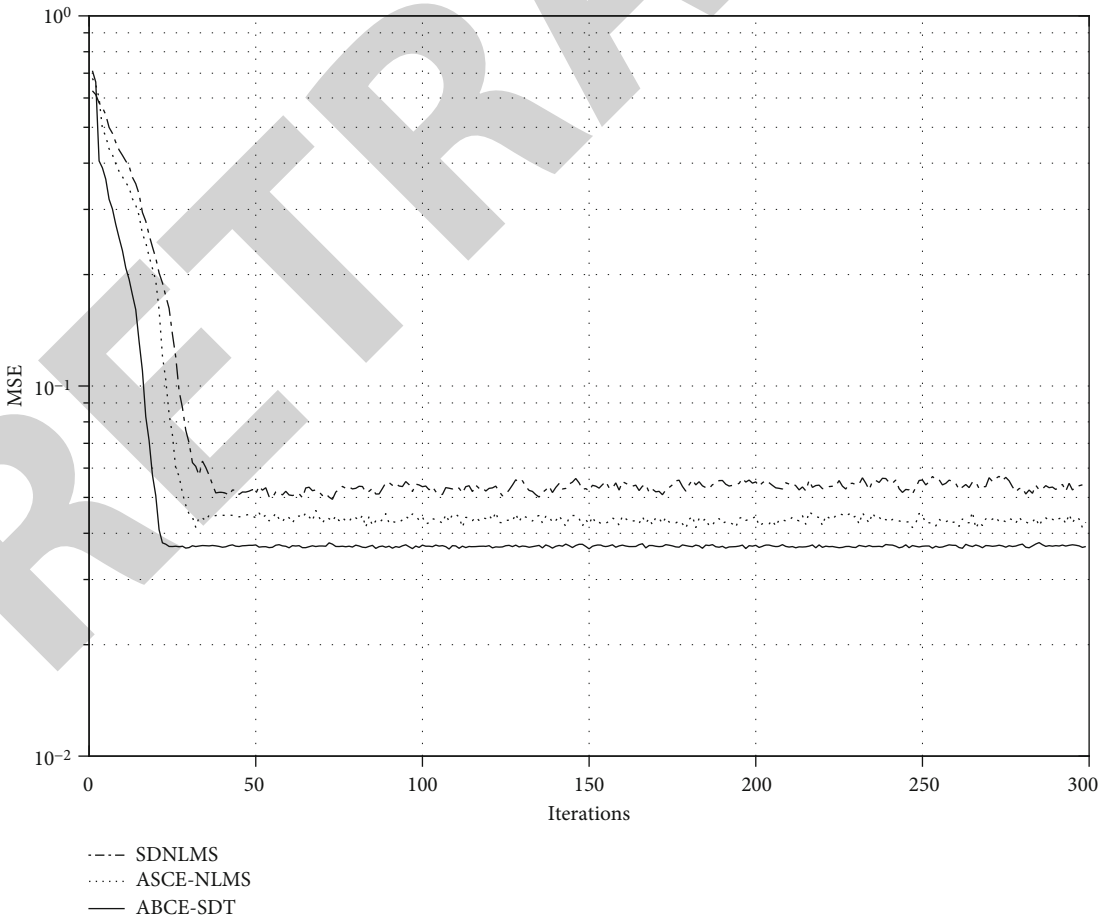

Figure 6: Channel tracking performances with linearly change channel.

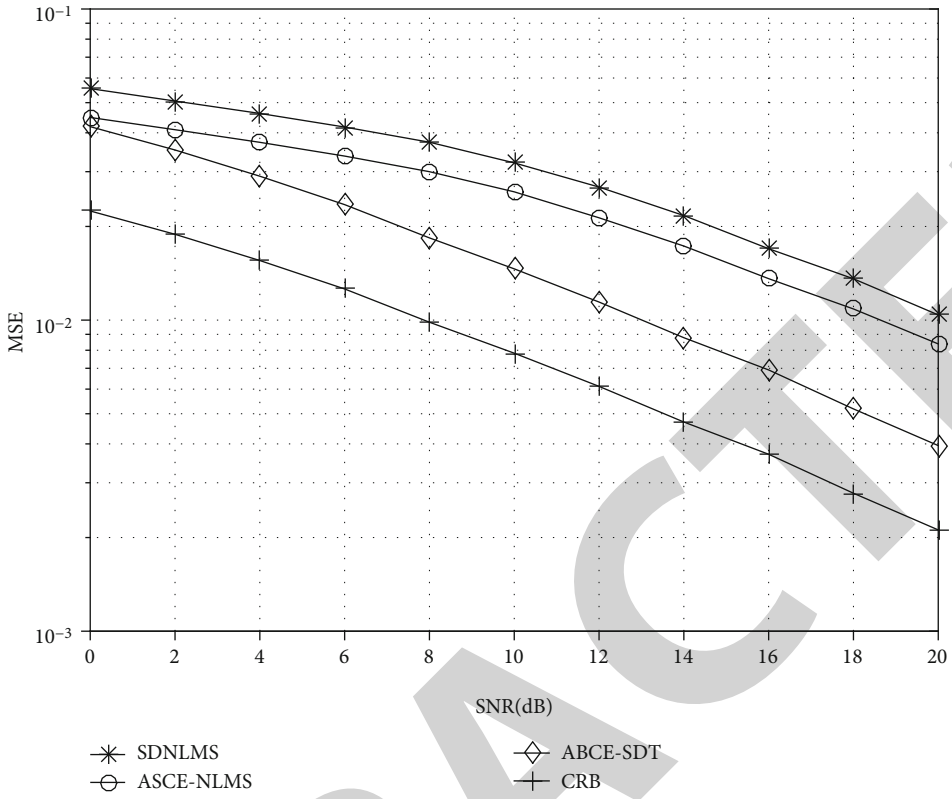

Figure 7: Channel estimation performances with linearly changing channel.

Therefore, estimation of channel and signals are obtained as $\widehat{\mathbf{H}}(k+1)$ and $\widehat{\mathbf{S}}(k+1)$, respectively. We present the pseudocode of the proposed adaptive channel estimation algorithm for MIMO-OFDM systems in Algorithm 1.

4. Simulation Results

In this section, we evaluate the performance of the proposed method. We provide simulation results under three different scenarios. In the first simulation, we test the proposed algorithm and the other two existing algorithms under a stationary environment exhibiting abrupt changes; in the second one, we consider the performance of the proposed method under a more realistic case of a slowly changing environment. In all cases, we consider the MSE as a measure of performance. The MSE is defined as

$$\mathrm{MSE}(k) = E\left\{\left\|\mathbf{H}(k) - \widehat{\mathbf{H}}(k)\right\|_2^2\right\}, \tag{31}$$

where $\mathbf{H}(k)$ and $\widehat{\mathbf{H}}(k)$ are true channel parameter matrix and their estimates, respectively. The kth received signal at the jth antenna writes $\tilde{\mathbf{X}}_j(k) = \mathbf{F}^H \boldsymbol{\Gamma} \boldsymbol{D}_j(\mathbf{H})\mathbf{s}(k) + \mathbf{n}_j(k)$ in noisy environment, where $\mathbf{n}_j(k)$ represents the additive noise in the jth antenna. Then, SNR is defined as

$$\mathrm{SNR} = 10\log_{10}\frac{\sum_{j=1}^{M_r}\left\|\mathbf{F}^H \boldsymbol{\Gamma} \boldsymbol{D}_j(\mathbf{H})\mathbf{s}\right\|_F^2}{\sum_{j=1}^{M_r}\left\|\mathbf{n}_j\right\|_F^2}\,\mathrm{dB}. \tag{32}$$

We drop the dependency of the SNR with k in the definition, which is because we use the same SNR for all OFDM symbols.

4.1. Abruptly Changing Environment. Here, we employ a MIMO-OFDM system with 2×3 antennas; the number of subcarriers is set to 32. The modulation scheme used is 16QAM; the length of Cyclic Prefix is set to 4. We use $J(k) = 200$ symbols to form the initial received symbols. The forgetting factor λ is 0.5. AWGN noise is added to the simulated MIMO-OFDM system and SNR = 10dB. We compare the channel estimation performance of the proposed ABCE-SDT algorithm and methods in [15, 20] with receive symbols vary from 200 to 1200, which can be seen in Figure 2. The step-size μ_s of the SDNLMS algorithm in [15] and the ASCE-NLMS algorithm in [20] is both set to 0.5. We use the IEEE 802.11 Model in the simulation. The simulated channel has the following structure; the power delay spectrum obeys negative exponential distribution.

$$E\left\{|h_l|^2\right\} = \exp\left(-l/10\right), l = 0, 1, \cdots, L, \tag{33}$$

where $L = 4$. Firstly, we can obtain a random channel response by the simulated channel model. We start with the channel response, and at iteration 501, we abruptly switch a new response obtained by the simulated channel model. We use OFDM symbols to measure time, especially, during the intervals $[0 \quad 500]$ and $[501 \quad 1000]$; we let the channel remains static.

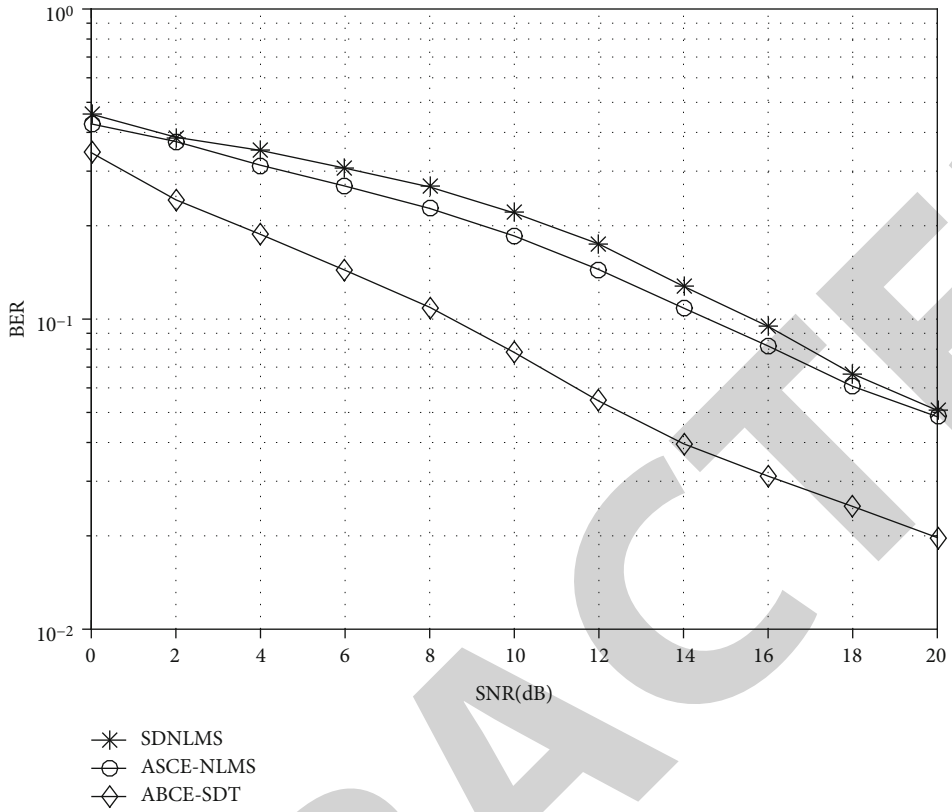

Figure 8: BER performances with linearly changing channel.

Figure 2 presents the channel tracking performance of the proposed ABCE-SDT algorithm, SDNLMS algorithm, and ASCE-NLMS algorithm. Obviously, the proposed ABCE-SDT method has higher MSE than other two methods at first, but it can achieve better performance soon, and it provides faster convergence. This is because the SDNLMS algorithm and ASCE-NLMS algorithm use training sequence to obtain the initial channel information whereas the ABCE-SDT method is blind. The window we used makes full use of all previously observed slices with different weights, which can speed up the convergence at low error. The other two algorithms only rely on the last observations; more symbols are needed to converge. The complexities of the ABCE-SDT, SDNLMS, and ASCE-NLMS algorithms for one iteration are $O(N^3M_r^3)$, $O(2N^3M_r^3 + 2NM_r)$, and $O(3N^3M_r^3 + 3NM_r)$, respectively. Obviously, the proposed algorithm requires the least computational burden compared to the other two methods, which is satisfied with what simulation shows. When the tracking process gets stable, it can be seen that the above algorithms have stable MSE with the iterations. When we abruptly change parameters of channel, the SDNLMS and ASCE-NLMS algorithms obtain poorer MSE performance than the ABCE-SDT algorithm, and they need more iterations to converge, even when the tracking process get stable; the MSE of the two methods still keep higher value. That is because the performance of the two competitors has error accumulation; new estimations are obtained by updating the old ones. The saltation of channel parameters caused the two competitors hardly to obtain an accurate channel estimation, whereas the proposed algorithm can compute the parameters of channel directly.

Moreover, we use Cramer-Rao bound as a benchmark. We plot the performances of these three algorithms and the corresponding CRB [32] in Figure 3. This result indicates that MSEs of the proposed ABCE-SDT method are very close to the corresponding CRBs. In order to reveal the performance of the entire system from the perspective of error probability, after the channel can be tracked, Figure 4 illustrates the averaged BER performance of three algorithms over 100 independent trials. We can obtain that the BER of three competitors decreases with the growth of SNR. At BER of 10^{-1}, the proposed algorithm achieves an SNR gain of about 6 dB compared with the existing algorithms, which means that the ABCE-SDT method achieves better BER performance than the other two existing methods.

4.2. Slowly Changing Environment. Now, we consider a more realistic scenario where the channel changes every OFDM symbol. The simulated MIMO-OFDM has 2×3 antennas with $N = 32$ subcarriers. We also use $J(k) = 200$ symbols to form the initial receive symbols. The simulated channel consists of five equal power taps; we create the initial parameters of channel by the IEEE 802.11 Model; then, we change the parameters linearly. The modulation scheme used is 16QAM. The forgetting factor λ is 0.5. AWGN noise is added to the simulated MIMO-OFDM system and SNR = 10dB.

Firstly, we let the channel parameters change linearly in every OFDM symbol. The simulated system has 6 paths;

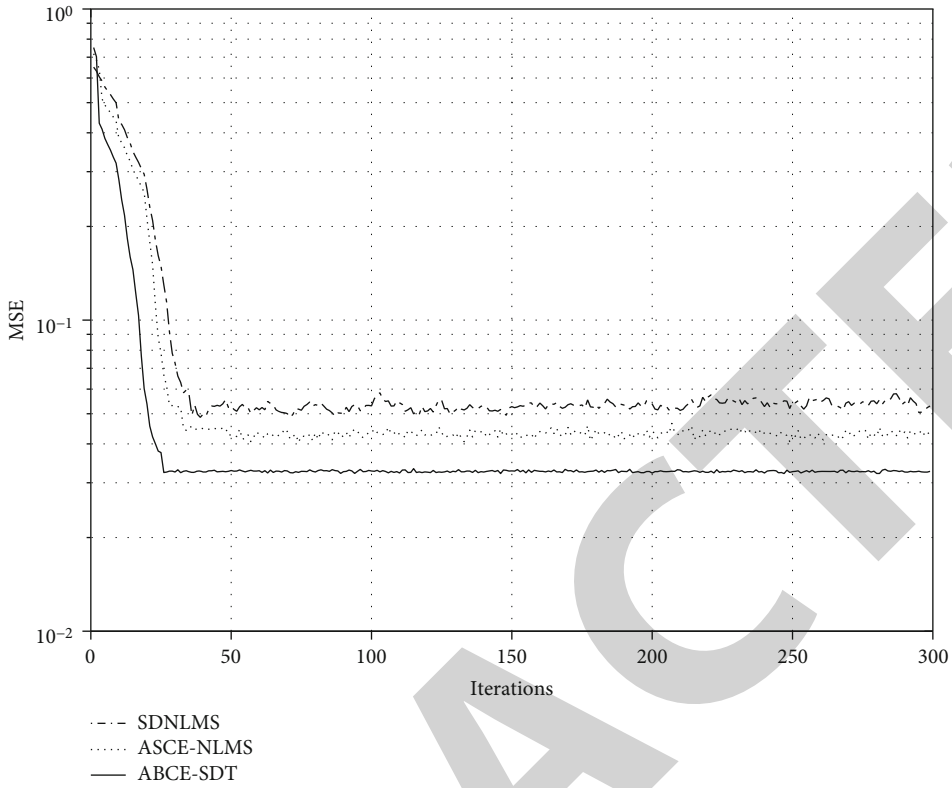

Figure 9: Channel tracking performances under fading channel.

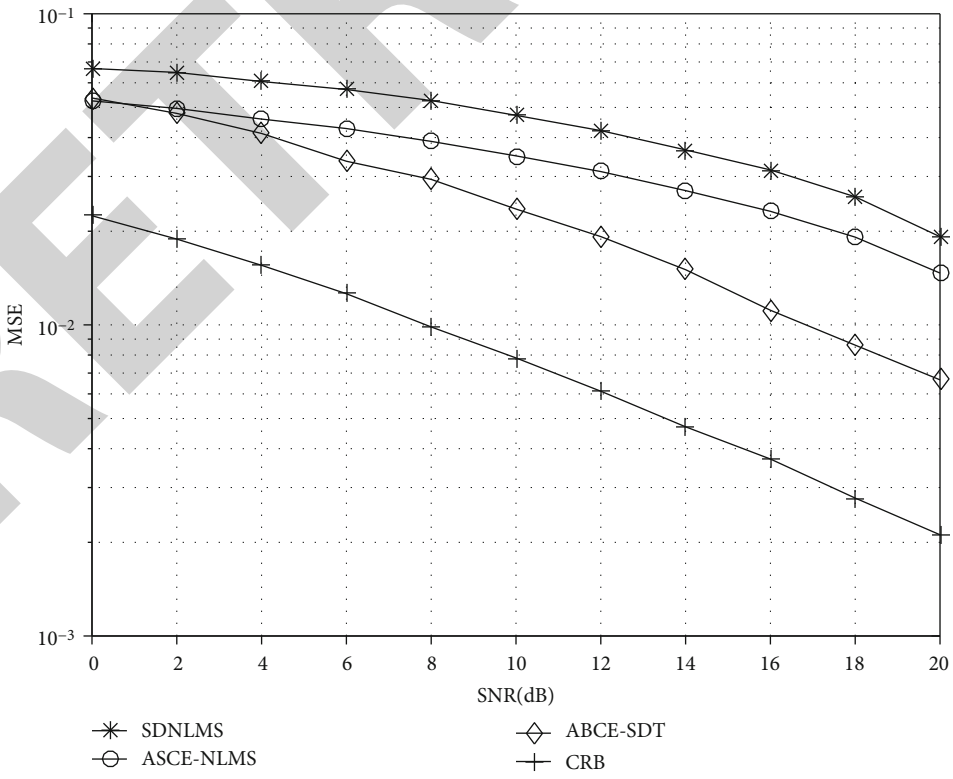

Figure 10: Channel estimation performances under fading channel.

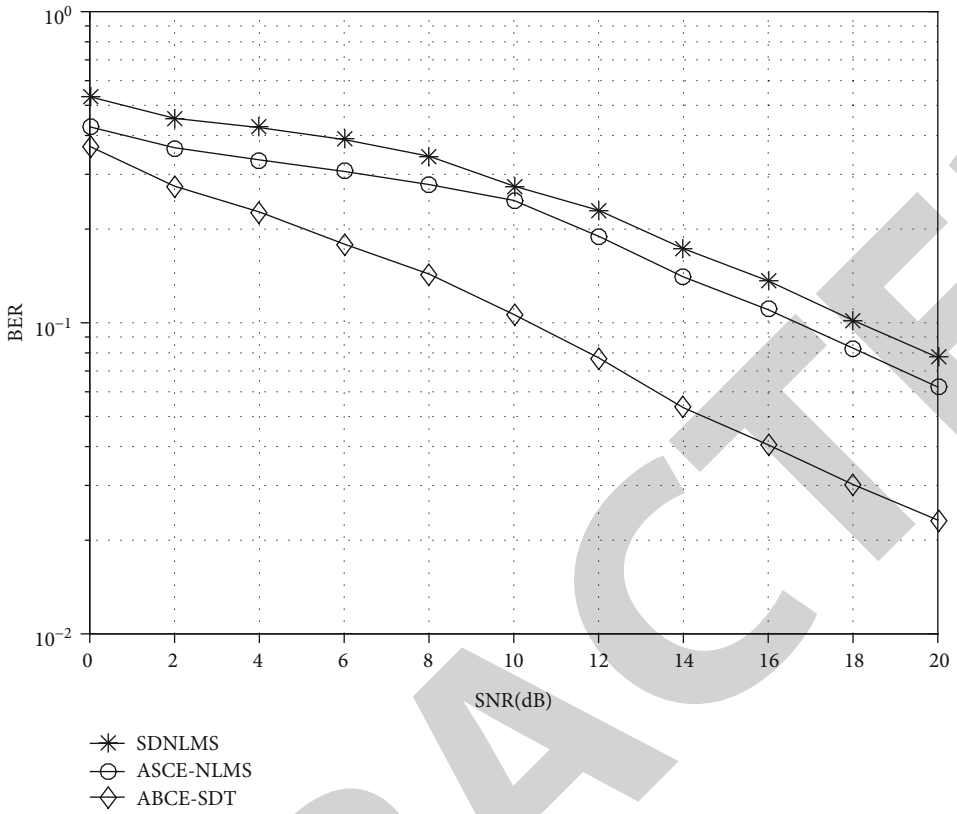

Figure 11: BER performances under fading channel.

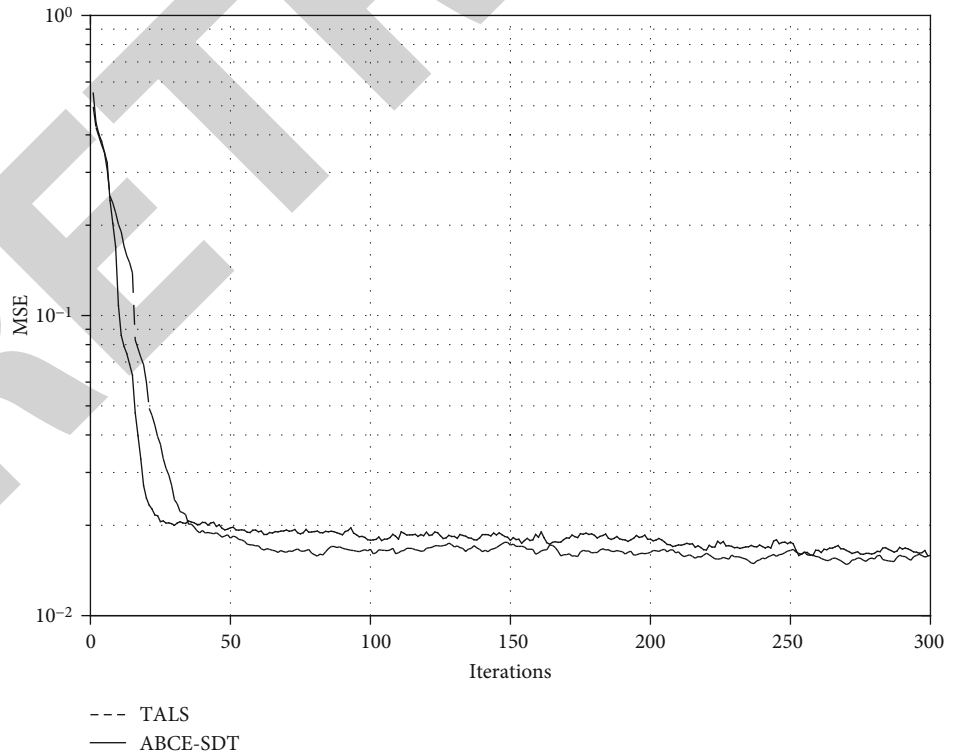

Figure 12: Channel tracking performances under the condition of CFO.

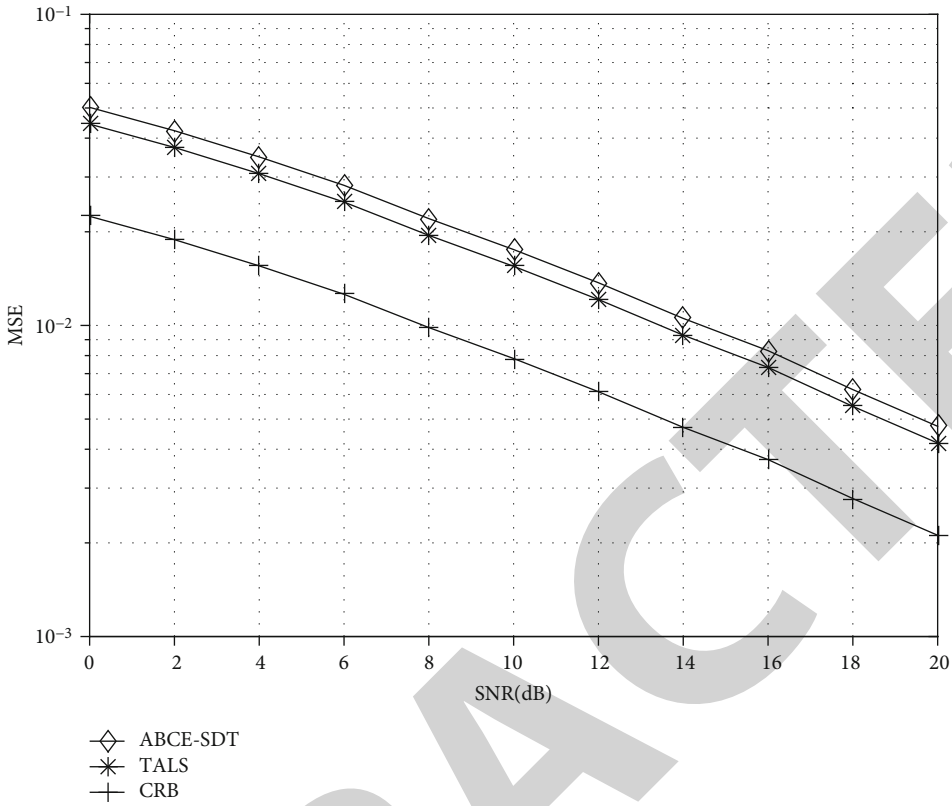

Figure 13: Channel estimation performances under the condition of CFO.

thus, we plot how the estimated channel tracked the real channel in Figures 5(a)–5(f). The labels of the x-axis and y-axis are real and imaginary of channel parameters, respectively. We can see the estimated channels have very close parameters with the real channels. In order to further verify the effectiveness, MSE performance of the proposed algorithm versus SDNLMS and ASCE-NLMS methods under the linear changed channel over 100 independent trials was shown in Figures 6 and 7. The step-size of the SDNLMS algorithm and ASCE-NLMS algorithm are both set as $\mu_s = 0.5$. In Figure 6, the ABCE-SDT method has higher MSE than the other two methods at first, but it can achieve better performance soon, and it provides faster convergence, which is close to the stationary environment with the stable channel. This is because the window we used makes full use of all previously observed slices with different weights, but the other two algorithms only rely on the last observations. It can also be observed that the SDNLMS and ASCE-NLMS algorithms perform a much higher fluctuation when channel can be tracked. Figure 8 represents the corresponding BER performance of the three competitors. Obviously, with the growth of SNR, the BER of three competitors decreases. At the BER of 10^{-1}, the proposed algorithm outperforms the SDNLMS and the ASCE-NLMS algorithms by about 6 dB and 8 dB SNR gains, respectively. Hence, the proposed ABCE-SDT algorithm achieves better BER performance than the other two algorithms.

Then, we examine the proposed algorithm under the fading channel. To simulate Rayleigh fading, here, we use a Jakes-like model; Doppler-frequency is 100 Hz and communication frequency carrier is at 5 GHz, with the data rate and receiver speed are at 2 Mbits/sec and 3 m/sec, respectively. The simulated channel consists of three equal power taps, and the power delay spectrum obeys negative exponential distribution. The simulated channel consists of five equal power taps, and the power delay spectrum obeys negative exponential distribution; the delay of each path is $[0 \quad 2e-6 \quad 4e-6 \quad 8e-6 \quad 12e-6]$. MSE performance of the ABCE-SDT method versus the SDNLMS and ASCE-NLMS methods under fading channel over 100 independent trials was shown in Figures 9 and 10. It can be seen that the ABCE-SDT method has a lower estimation error and provides faster convergence under fading channel. The high fluctuation of SDNLMS and ASCE-NLMS still exists when the channel can be tracked. We also plot the corresponding BER performance of the three algorithms after channel can be tracked in Figure 11. Obviously, the proposed ABCE-SDT method achieves better BER performance than the other two competitors under the fading channel.

4.3. Carrier Frequency Offset Environment. Furthermore, we take the effect of carrier frequency offset (CFO) on the channel estimation algorithms into consideration. The simulated MIMO-OFDM has 2×3 antennas with $N = 32$ subcarriers. We also use $J(k) = 200$ symbols to form the initial receive symbols. Each tap of the simulated channel is modeled as an independent complex Gaussian random variable, and here, we set the number of channel taps as 5. The carrier

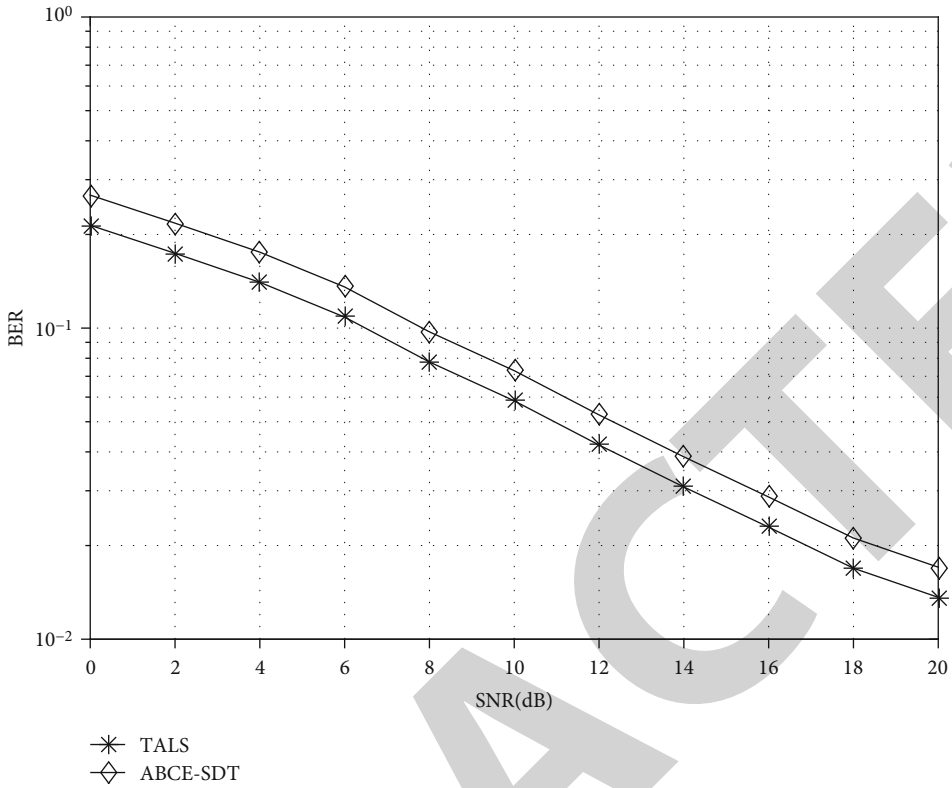

Figure 14: BER performances under the condition of CFO.

frequency offset ϕ is set as $\phi = 0.02\Delta\omega$, where $\Delta\omega = 2\pi/N$ is the subcarrier spacing. The modulation scheme used is 16QAM. The forgetting factor λ is 0.9. The signal to noise ratio SNR = 10dB, and AWGN noise was used in simulation.

We set the channel parameters to stay unchanged during one OFDM symbol, and changes linearly vary for different OFDM symbols. We use the Rayleigh fading channel for simulation. We plot in Figures 12 and 13 the MSE performance of the proposed algorithm versus TALS methods in [24] under the linear changed channel over 100 independent trials. We can find out that the proposed method performs almost the same MSE with the TALS method, and it provides faster convergence. In fact, the computation complexity of the TALS algorithm is $O(3N^3M_r^3)$ every time iteration, and it needs almost 20 times iteration to reach the convergence condition. Figure 14 represents the corresponding BER performance of the other two competitors. Similarly, with the growth of SNR, the BER of three competitors decrease. As Figure 14 shows, due to lower estimation error, the TALS method achieves a bit better BER performance than the proposed algorithm. Whereas, the TALS algorithm needs pseudoinverse operation three times at each iteration, and the convergence speed is slow even with a proper initialization. The proposed ABCE-SDT algorithm can obtain faster convergence speed at the loss of little performance decrease.

5. Conclusion

Adaptive channel estimation is necessary for tracking the channel under wireless random time-varying conditions in MIMO-OFDM systems. In this paper, we propose an adaptive blind channel estimation method based on PARAFAC; the pilot sequence is not needed in the proposed ABCE-SDT method. We used an exponential window to weight the past observations; thus, the cost function can be constructed via a weighted least squares criterion. The minimization of the cost function is equivalent to the decomposition of third-order tensor which consists of the weighted OFDM data symbols. To reduce the computational load, we adopt a recursive singular value decomposition method for tensor decomposition; then, the channel parameters can be estimated adaptively. Computer simulations verify the effectiveness of the proposed algorithm under diverse signalling conditions.

Data Availability

The data used to support the fundings of this study are available from the corresponding author upon request.

Conflicts of Interest

The authors declare that there are no conflicts of interest regarding the publication of this paper.

Acknowledgments

The authors greatly appreciate the editor and reviewers for their work. This work was funded by the National Natural Science Foundation of China by Grant 62071350 and by

the Science and Technology Research Program of Shaanxi Province under Grant 2018KJXX-019.

References

[1] S. B. Ramteke, A. Y. Deshmukh, and K. N. Dekate, "A Review on Design and Analysis of 5G Mobile Communication MIMO System with OFDM," in *2018 Second International Conference on Electronics, Communication and Aerospace Technology (ICECA)*, pp. 542–546, Coimbatore, India, March 2018.

[2] H. Kaur, M. Khosla, and R. K. Sarin, "Channel Estimation in MIMOOFDM System: A Review," in *2018 Second International Conference on Electronics, Communication and Aerospace Technology (ICECA),*, pp. 974–980, Coimbatore, India, March 2018.

[3] Y. Zhang, D. Wang, J. Wang, and X. You, "Channel estimation for massive MIMO-OFDM systems by tracking the joint angle-delay subspace," *IEEE Access*, vol. 4, pp. 10166–10179, 2016.

[4] E. P. Simon and M. A. Khalighi, "Iterative soft-Kalman channel estimation for fast time-varying MIMO-OFDM channels," *IEEE Wireless Communications Letters*, vol. 2, no. 6, pp. 599–602, 2013.

[5] Z. Yuan, C. Zhang, Z. Wang, Q. Guo, and J. Xi, "An auxiliary variable-aided hybrid message passing approach to joint channel estimation and decoding for MIMO-OFDM," *IEEE Signal Processing Letters*, vol. 24, no. 1, pp. 12–16, 2017.

[6] B. Aly, "Performance analysis of adaptive channel estimation for UOFDM indoor visible light communication," in *2016 33rd National Radio Science Conference (NRSC)*, pp. 217–222, Aswan, Egypt, February 2016.

[7] B. S. Chen, C. Y. Yang, and W. J. Liao, "Robust fast time-varying multipath fading channel estimation and equalization for MIMO-OFDM systems via a fuzzy method," *IEEE Transactions on Vehicular Technology*, vol. 61, no. 4, pp. 1599–1609, 2012.

[8] H. Hojatian, M. J. Omidi, H. Saeedi-Sourck, and A. Farhang, "Joint CFO and channel estimation in OFDM-based massive MIMO systems," in *The 8th International Symposium on Telecommunications (IST)*, pp. 343–348, Tehran, Iran, September 2016.

[9] D. Li, S. Feng, and W. Ye, "Pilot-assisted channel estimation method for OFDMA systems over time-varying channels," *IEEE Communications Letters*, vol. 13, no. 11, pp. 826–828, 2009.

[10] H. Zamiri-Jafarian and G. Gulak, "Adaptive channel SVD estimation for MIMO-OFDM systems," in *IEEE 61st Vehicular Technology Conference*, vol. 1, pp. 552–556, Stockholm, Sweden, June 2005.

[11] W. C. Chen and C. D. Chung, "Spectrally efficient OFDM pilot waveform for channel estimation," *IEEE Transactions on Communications*, vol. 65, no. 1, pp. 1–402, 2016.

[12] X. Dai, H. Zhang, and D. Li, "Linearly time-varying channel estimation for MIMO/OFDM systems using superimposed training," *IEEE Transactions on Communications*, vol. 58, no. 2, pp. 681–693, 2010.

[13] Z. Tang, R. C. Cannizzaro, G. Leus, and P. Banelli, "Pilot-assisted time-varying channel estimation for OFDM systems," *IEEE Transactions on Signal Processing*, vol. 55, no. 5, pp. 2226–2238, 2007.

[14] E. H. Krishna, K. Sivani, and K. A. Reddy, "OFDM channel estimation using novel LMS adaptive algorithm," in *International Conference on Computer, Communication and Signal Processing (ICCCSP)*, pp. 1–5, Chennai, India, January 2017.

[15] T. A. Dewan, S. Hasan, and F. Hossain, "Low complexity SDNLMS Adaptive Channel Estimation for MIMO-OFDM systems," in *2013 International Conference on Electrical Information and Communication Technology (EICT)*, pp. 1–5, Khulna, Bangladesh, March 2014.

[16] Die Hu, Xiaodong Wang, and Lianghua He, "A new sparse channel estimation and tracking method for time-varying OFDM systems," *IEEE Transactions on Vehicular Technology*, vol. 62, no. 9, pp. 4648–4653, 2013.

[17] X. Ma, F. Yang, S. C. Liu, J. Song, and Z. Han, "Sparse channel estimation for MIMO-OFDM systems in high-mobility situations," *IEEE Transactions on Vehicular Technology*, vol. 67, no. 7, pp. 6113–6124, 2018.

[18] Q. B. Qin, L. Gui, B. Gong, and S. Luo, "Sparse channel estimation for massive MIMO-OFDM systems over time-varying channels," *IEEE Access*, vol. 6, pp. 6113–6124, 2018.

[19] G. Qiao, Q. Song, L. Ma, S. Liu, Z. Sun, and S. Gan, "Sparse Bayesian learning for channel estimation in time-varying underwater acoustic OFDM communication," *IEEE Access*, vol. 6, pp. 56675–56684, 2018.

[20] G. Gui and F. Adachi, "Stable adaptive sparse filtering algorithms for estimating multiple-input-multiple-output channels," *IET Communications*, vol. 8, no. 7, pp. 1032–1040, 2014.

[21] X. G. Doukopoulos and G. V. Moustakides, "Blind adaptive channel estimation in OFDM systems," *IEEE Transactions on Wireless Communications*, vol. 5, no. 7, pp. 1716–1725, 2006.

[22] A. Y. Kibangou and G. Favier, "Non-iterative solution for PARAFAC with a Toeplitz matrix factor," *17th European Signal Processing Conference*, 2009, pp. 691–695, Glasgow, UK, August 2009.

[23] Z. Xiaofei, W. Fei, and X. Dazhuan, "Blind signal detection algorithm for MIMO-OFDM systems over multipath channel using PARALIND model," *IET Communications*, vol. 5, no. 5, pp. 606–611, 2011.

[24] T. Jiang and N. D. Sidiropoulos, "A direct blind receiver for SIMO and MIMO OFDM systems subject to unknown frequency offset and multipath," in *2003 4th IEEE Workshop on Signal Processing Advances in Wireless Communications - SPAWC 2003 (IEEE Cat. No.03EX689)*, pp. 358–362, Rome, Italy, June 2003.

[25] M. Rajih, P. Comon, and D. Slock, "A deterministic blind receiver for MIMO OFDM systems," in *2006 IEEE 7th Workshop on Signal Processing Advances in Wireless Communications*, pp. 1–5, Cannes, France, July 2006.

[26] K. Liu, J. P. C. L. da Costa, H. C. So, and A. L. F. de Almeida, "Semi-blind receivers for joint symbol and channel estimation in space-time-frequency MIMO-OFDM systems," *IEEE Transactions on Signal Processing*, vol. 61, no. 21, pp. 5444–5457, 2013.

[27] F. Wen, J. Shi, and Z. Zhang, "Joint 2D-DOD, 2D-DOA, and polarization angles estimation for bistatic EMVS-MIMO radar via PARAFAC analysis," *IEEE Transactions on Vehicular Technology*, vol. 69, no. 2, pp. 1626–1638, 2020.

[28] D. Nion and N. D. Sidiropoulos, "Adaptive algorithms to track the PARAFAC decomposition of a third-order tensor," *IEEE Transactions on Signal Processing*, vol. 57, no. 6, pp. 2299–2310, 2009.

[29] V.-D. Nguyen, K. Abed-Meraim, and L.-T. Nguyen, "Fast adaptive PARAFAC decomposition algorithm with linear complexity," in *2006 nternational Conference on Acoustics, Speech and Signal Processing (ICASSP)*, pp. 6235–6239, Shanghai, China, March 2016.

[30] P. Strobach, "Bi-iteration SVD subspace tracking algorithms," *IEEE Transactions on signal processing*, vol. 45, no. 5, pp. 1222–1240, 1997.

[31] Y. Zi and Y. M. Cai, "Cramer-rao bound for blind, semi-blind and non-blind channel estimation in ofdm systems," in *IEEE International Symposium on Communications & Information Technology*, pp. 523–526, Beijing, China, January 2006.